The GROMOS Software for (Bio)Molecular Simulation

Volume 1: About the GROMOS package: Overview

January 9, 2021

Contents

CHAPTER 1

What is GROMOS

GROMOS is an acronym of the GROningen MOlecular Simulation computer program package, which has been developed since 1978 for the *dynamic modelling of (bio)molecules*, until 1990 at the University of Groningen, The Netherlands, and since then at the ETH, the Swiss Federal Institute of Technology in Zürich, Switzerland. Until 2013 its development was driven by the research group of Wilfred van Gunsteren. Currently, the development is shared between him and the research groups of Philippe Hünenberger and Sereina Riniker at the ETH and of Chris Oostenbrink at the Institute for Molecular Modeling and Simulation of the University of Natural Resources and Life Sciences in Vienna, Austria.

Since the last official release of the GROMOS software and manual in 1996, called GROMOS96, no comprehensive release occurred till 2011. Yet the GROMOS software has seen a steady development since 1996, see e.g. Christen *et al.* J. Comput. Chem. **26** (2005) 1719. The programming language has been changed from FORTRAN to C++, the documentation has been put into electronic form, and many new features have been included in the software. In spring 2011 an official version of the C++ software was released and this volume summarizes the basic principles underlying the development of the GROMOS software.

The GROMOS software has been developed as a research vehicle of the van Gunsteren research group, which was characterized by a changing composition of members that are interested in both methodological developments and a variety of applications of simulation methods. This dictated the following principles for development:

- Transparency of code, so that modification is easy.
- Molecular architecture, so that parts of it can be used in changing combinations and functions may be replaced by ones written by the user.
- Independence of the code of the force field that is used.
- Independence of the code of the units of physical quantities and constants.
- Independence of the code of the computer hardware that is available.

The criteria for inclusion of new features into GROMOS are, ordered according to decreasing importance:

1. Research and teaching interests of the research groups developing the code.
2. Scientific importance
3. Demonstrated usefulness or efficiency
4. Well-defined and correct formulae and algorithms
5. Extent of use by the scientific community
6. Ease of implementation
7. Computational efficiency

CHAPTER 2

The GROMOS force fields

The GROMOS software is to be distinguished from the GROMOS force fields for biomolecular systems.

The quality of the interaction function or force field that describes the forces between the atoms of a biomolecular system is of decisive importance for the predictive power of MD simulations. Therefore, we have over the past decades spent much effort to gradually improve the GROMOS force field whenever results of simulation applications pointed at force field deficiencies. The first set of non-bonded GROMOS force field parameters dates from 1984,[1] while the bonded parameters were taken from ref.[2]. Since then, the force field has continuously been improved and refined.[3–15] The most widely used versions of the GROMOS force field are the GROMOS 37C4 force field of 1985, the GROMOS 43A1 force field of 1996[4,16] and the GROMOS 45A3 force field of 2001.[6] The currently used versions are the 45A4 parameter set,[7,9,10] the 53A5/6,[8] the 54A7,[12,14] and the 54A8 one.[15] In parallel to the development of force field parameters for biomolecules, solvent models that are consistent with the GROMOS biomolecular force field were developed for much used (co-)solvents:[17] water,[18,19] methanol,[20] DMSO,[21] chloroform,[22] carbontetrachloride,[23] urea,[24] acetonitrile.[25] A polarisable force field is under development,[26–37] as are supra-molecular coarse-grained ones for water[38–40], co-solvents[41–43] and lipids.

CHAPTER 3

GROMOS functionalities and documentation

GROMOS has the following *basic capabilities*.

1. Simulation of biomolecules or arbitrary molecules using the molecular dynamics (MD) or stochastic dynamics (SD) methods.
2. Analysis of molecular configurations and velocities or energies obtained by computer simulation or model building based on experimental (X-ray, NMR) data.

The GROMOS software manuals that accompanied the major releases of 1987 and 1996 are

W.F. van Gunsteren and H.J.C. Berendsen
Groningen Molecular Simulation (GROMOS) Library Manual
Biomos, Groningen, The Netherlands, 1987, pp. 1-221

W.F. van Gunsteren , S.R. Billeter, A.A. Eising, P.H. Hünenberger, P. Krüger, A.E. Mark, W.R.P. Scott and I.G. Tironi
Biomolecular Simulation: The GROMOS96 Manual and User Guide
Vdf Hochschulverlag AG an der ETH Zürich, Zürich, Switzerland, 1996, pp. 1-1042

The current GROMOS manual and user guide exists of 9 volumes:

The GROMOS Software for (Bio)Molecular Simulation
Volume 1: About the GROMOS Package: Overview
Volume 2: Algorithms and Formulae for Modelling of Molecular Systems
Volume 3: Force Field and Topology Data Set
Volume 4: Data Structures and Formats
Volume 5: Program Library Manual
Volume 6: Technical Details
Volume 7: Tutorial with Examples
Volume 8: Installation Guide
Volume 9: Index

The functionalities of GROMOS 87, GROMOS96 and GROMOS 05 have been summarized in

- W.R.P. Scott and W.F. van Gunsteren
  The GROMOS Software Package for Biomolecular Simulations
  In: Methods and Techniques in Computational Chemistry: METECC-95, E. Clementi and G. Corongiu editors, STEF, Cagliari, Italy, 1995, pp. 397-434.
- W.R.P. Scott, P.H. Hünenberger, I.G. Tironi, A.E. Mark, S.R. Billeter, J. Fennen, A.E. Torda, T. Huber, P. Krüger and W.F. van Gunsteren
  The GROMOS Biomolecular Simulation Package
  J. Phys. Chem. A 103 (1999) 3596-3607
- M. Christen, P.H. Hünenberger, D. Bakowies, R. Baron, R. Bürgi, D.P. Geerke, T.N. Heinz, M.A. Kastenholz, V. Kräutler, C. Oostenbrink, C. Peter, D. Trzesniak and W.F. van Gunsteren
  The GROMOS Software for Biomolecular Simulation: GROMOS 05
  J. Comput. Chem. 26 (2005) 1719-1751

The architecture and different functionalities of the current version of GROMOS, GROMOS 11, are described in the following papers:

- N. Schmid, C.D. Christ, M. Christen, A.P. Eichenberger and W.F. van Gunsteren
  Architecture, Implementation and Parallelisation of the GROMOS Software for Biomolecular Simulation
  Comp. Phys. Commun. 183 (2012) 890-903
- A.P.E. Kunz, J.R. Allison, D.P. Geerke, B.A.C. Horta, P.H. Hünenberger, S. Riniker, N. Schmid and W.F. van Gunsteren
  New Functionalities in the GROMOS Biomolecular Simulation Software
  J. Comput. Chem. 33 (2012) 340-353
- S. Riniker, C.D. Christ, H.S. Hansen, P.H. Hünenberger, C. Oostenbrink, D. Steiner and W.F. van Gunsteren
  Calculation of Relative Free Energies for Ligand-Protein Binding, Solvation and Conformational Transitions using the GROMOS Biomolecular Simulation Software
  J. Phys. Chem. B 115 (2011) 13570-13577
- N. Schmid, J.R. Allison, J. Dolenc, A.P. Eichenberger, A.P.E. Kunz, and W.F. van Gunsteren
  Biomolecular Structure Refinement using the GROMOS Simulation Software
  J. Biomol. NMR 51 (2011) 265-281
- A.P. Eichenberger, J.R. Allison, J. Dolenc, D.P. Geerke, B.A.C. Horta, K. Meier, C. Oostenbrink, N. Schmid, D. Steiner, D. Wang and W.F. van Gunsteren
  The GROMOS++ Software for the Analysis of Biomolecular Simulation Trajectories
  J. Chem. Theory Comput. 7 (2011) 3379-3390
- S.J. Bachmann, W.F. van Gunsteren
  On the compatibility of polarisable and non-polarisable models for liquid water
  Mol. Phys. 112 (2014) 2761-2780
- N. Hansen, F. Heller, N Schmid, W.F. van Gunsteren
  Time-averaged order parameter restraints in molecular dynamics simulations
  J. Biomol. NMR 60 (2014) 169-187

The GROMOS C++ code is documented in the code in the form of a doxygen documentation. It is accompanied by make files, etc. and by example files.

CHAPTER 4

Examples of application of GROMOS

During the past forty years the computer has taken an increasingly prominent position in science. This is due to the rapid increase of computer power. Every five to six years the ratio of performance to price has increased by a factor of ten. This development has paved the way for simulating in atomic detail a variety of physical processes on a computer. Computer simulation is a powerful tool to predict molecular properties that are inaccessible to experiments once the reliability of the molecular models, force fields and computational procedures has been established by comparison of simulated properties with known experimental ones. This may lead to the design of substances or molecules that possess specific properties useful in practical applications. Here, one may think of applications in drug or vaccine design, in protein engineering or in material science. The common approach to modelling a molecular system on a computer is a static one. For example, quantum calculations yield a particular charge distribution; Molecular Mechanics calculations yield one or a few minimum energy conformations of a molecule; on a graphics device molecules are studied in terms of fixed conformations.

However, a molecular system at room temperature is by no means of static character. A system of interacting atoms traverses multiple minima of the potential energy surface. One would like to know the multidimensional distribution function of all atomic coordinates and its development in time. This knowledge can never be complete. Only parts of configuration space can be searched for relevant low (free) energy conformations. The computer simulation technique of Molecular Dynamics provides the possibility to scan that part of configuration space that is accessible to the molecular system at the given temperature.

Static modelling techniques are completely inadequate to describe the properties of a system in a number of applications. Examples are the behaviour of liquid water and its influence on the conformation of a solute, and the calculation of quantities like entropy and free energy. The latter determine such properties as the binding strength of small drug molecules to large acceptor molecules, which is crucial in the process of drug design.

Dynamic modelling techniques are therefore a very promising tool in the field of (bio)molecular chemistry and physics. Below we sketch a few applications of the GROMOS software and force fields.

4.1. Analysis: Calculation of dielectric permittivity and relaxation time

The static dielectric permittivity $\epsilon(0)$ and the Debye relaxation time τ_D of a molecular liquid can be obtained from non-equilibrium MD simulations of the liquid in which a homogeneous static external electric field $\mathbf{E}^{ext}$ is switched on at $t = t_0$.[44] Upon switching on $\mathbf{E}^{ext}$ along the z-axis at $t = t_0$, the z-component P_z of the polarisation $\mathbf{P}$ will increase from its initial value $P_z(t_0)$, which values are Gaussian distributed around $P_z = 0$, to a steady-state value $P_z(t = \infty)$. For a Debye dielectric medium, this build-up will be exponential,

$$\langle P_z(t)\rangle_{t_0} = \langle P_z(t=\infty)\rangle_{t_0}\left[1 - e^{-(t-t_0)/\tau_P}\right]. \tag{4.1}$$

The value of $P_z(t = \infty)$ will be larger for larger E_z^{ext}, but different field strengths E_z^{ext} should yield the same τ_P, as long as E_z^{ext} is not too small and not too large. The static dielectric permittivity of the molecular model is then

$$\epsilon(0) = 1 + 4\pi\frac{P_z(t=\infty)}{E_z^{ext}} \tag{4.2}$$

and the Debye relaxation time is

$$\tau_D = \frac{\epsilon(0) + 2 + C_{rf}(\epsilon(0) - 1)}{3}\tau_P \tag{4.3}$$

in which C_{rf} is a constant depending on the dielectric permittivity ϵ_{cs} of the medium inside the cut-off sphere with radius R_{rf} and the dielectric continuum outside the cut-off sphere is characterised by a dielectric permittivity ϵ_{rf} and an inverse Debye screening length κ_{rf} .

The results for three different system sizes of a cubic box of liquid simple-point-charge (SPC) water are shown in Tab. 4.1 and Fig. 4.1. While the variation of $P_z(t=\infty)$ decreases with increasing system size due to better statistics, the average relaxation is independent of system size, and so are the values obtained for τ_D and $\epsilon(0)$.

Number of H_2O	$\epsilon(0)$	E_z^{ext}	τ_D	E_z^{ext}	τ_D
1024	63	0.03	6.1	0.05	6.0
5384	67	0.03	6.6	0.05	6.0
12800	64	0.03	6.3	0.05	6.0

TABLE 4.1. Calculated values for the relative static dielectric permittivity $\epsilon(0)$ and the Debye dielectric relaxation time τ_D (ps) at 298 K and 1 atm for water using three different system sizes and two different electric field strengths.[44] The electric field strengths (enm^{-2}) were chosen such that they are as large as possible while being in the linear-response regime.

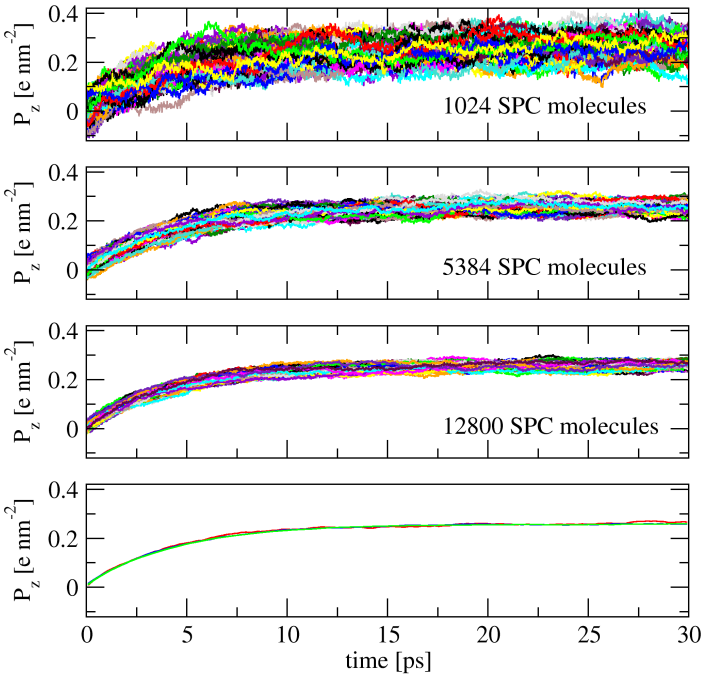

FIGURE 4.1. Polarisation $P_z(t)$ for 100 non-equilibrium MD simulations[44] of liquid water using three different system sizes, 1024, 5384 and 12800 SPC molecules, after switching on an electric field $E_z^{ext} = 0.05$ e nm^{-2} at $t_0 = 0$. The averages over the 100 trajectories are shown in red (1024 molecules), blue (5384 molecules) and green (12800 molecules) in the lowest panel.

4.2. Simulation of polypeptide folding using a polarisable solvent

Folding and unfolding of β-peptides has been studied extensively by molecular dynamics simulation. In these simulations, a non-polarisable model for the solvent, mostly methanol, was used. If a polarisable

solvent is used, the agreement with the experimental data from NMR is slightly improved, see Fig. 4.2. In the polarisable solvent the helical structure of the 7-residue β-peptide, which has a large dipole moment, is stabilised[45]. This means that the introduction of electronic polarisability into the solvent model appears of importance to a proper description of folding equilibria if these are determined by competing solute conformations that have different dipole moments.

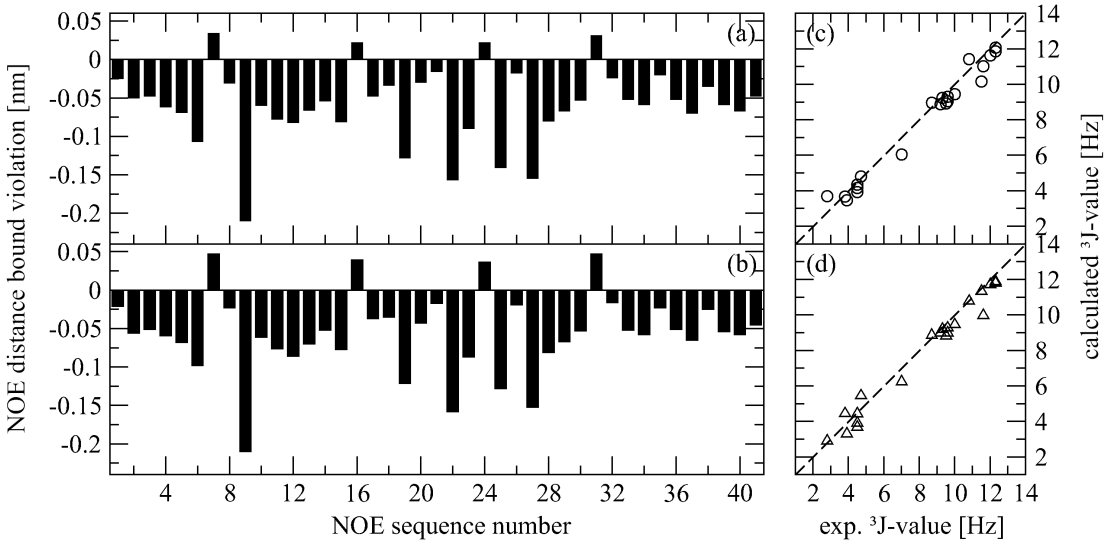

FIGURE 4.2. Comparison of r^{-6} averaged NOE distances and average ^3J-coupling constants as obtained from simulations (at 340 K, 1 atm) and experimental data of a 7-residue β-peptide.[45] Panels (a,c): in polarisable methanol (b,d): in non-polarisable methanol.

4.3. Properties of coarse-grained models for solvents: H_2O and co-solvents

The development of coarse-grained (CG) models that represent the important features of compounds is essential to overcome limitations in time scale and system size currently encountered in atomistic molecular dynamics simulations. Since the solvent interactions account for most of the computational effort in a biomolecular simulation, coarse-graining of the solvent model significantly enhances the efficiency of a simulation. In Fig. 4.3 and Fig. 4.4, some thermodynamic properties of mixtures of CG DMSO and CG MeOH with CG H_2O[38] are shown. Apart from the energy of mixing, the trends as function of mole fraction are reproduced. A change of DMSO-H_2O and MeOH-H_2O Lennard-Jones interaction would be sufficient to obtain negative values for ΔU_{mix}.

4.4. Enhancing the configurational sampling of ions

While configurational sampling of a liquid is relatively easy, due to the fact that it consists of many identical molecules that may exchange their position in space, the conformational sampling of a protein is much more difficult due to the connectivity of its covalent topology which impedes a fast exchange of atom positions. Sampling the configurational distribution of ions around a protein is a challenge that lies somewhere between these two cases. The sampling of ionic degrees of freedom can be considerably enhanced by using the technique of adiabatic decoupling the motion of the ionic degrees of freedom from that of the water solvent and then raising the temperature of the ions. The ionic diffusion turned out to be 15 times larger while keeping the distribution of the water molecules around the ions unaltered with respect to the standard temperature simulation, see Tab. 4.2.[46]

4.5. Calculation of protein-ligand binding free enthalpies

The relative free enthalpy of binding of different inhibitors to a protein can be obtained using enveloping distribution sampling (EDS), which is a computationally efficient alternative to the method of thermodynamic integration. In Fig. 4.5, the binding free enthalpies of three inhibitors of the protein

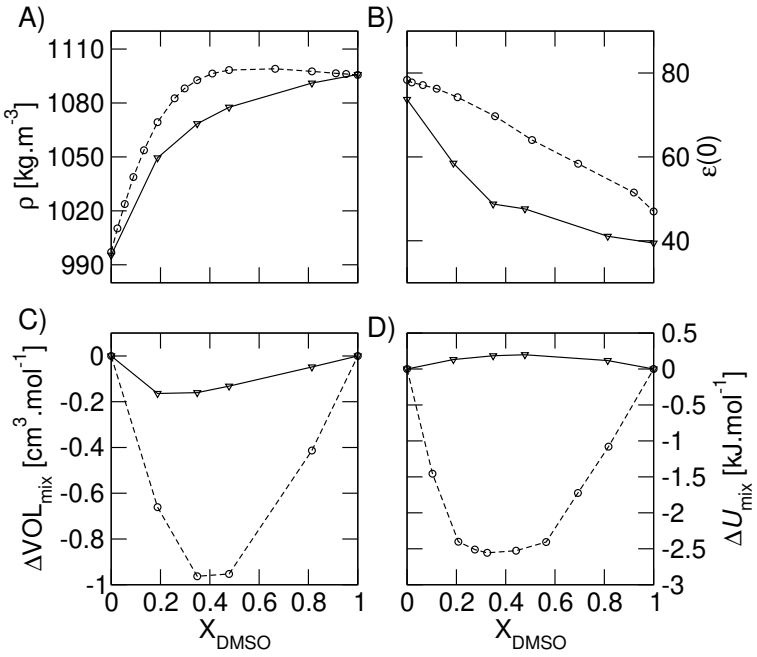

FIGURE 4.3. Thermodynamic properties of coarse-grained (CG) DMSO:H_2O mixtures at 298 K and 1 atm, as a function of the mole fraction of DMSO, X_{DMSO}, from MD simulations: (A) densities ρ, (B) dielectric permittivities $\epsilon(0)$, (C) excess volume of mixing ΔVOL_{mix} and (D) excess potential energy of mixing ΔU_{mix}. Experimental data are shown in solid lines and results of the CG simulations are in dashed lines.

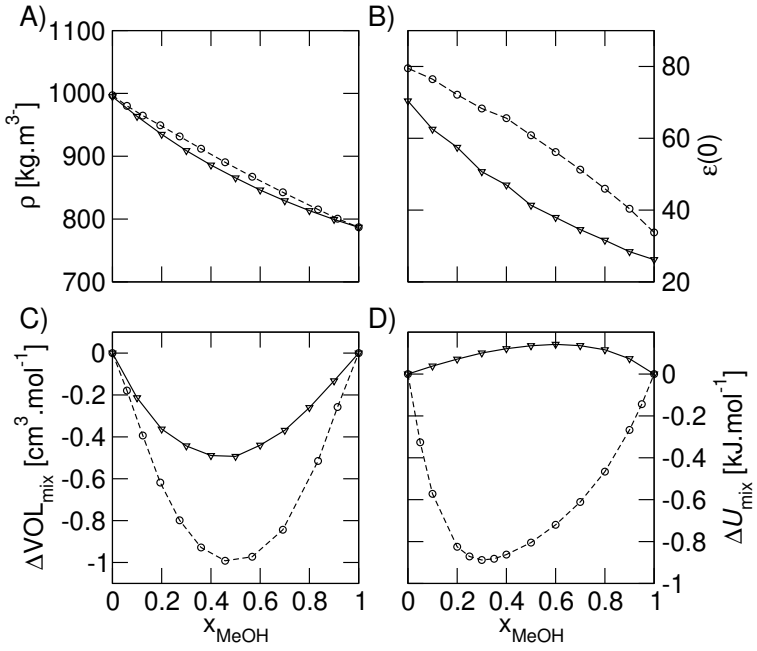

FIGURE 4.4. Thermodynamic properties of coarse-grained (CG) MeOH:H_2O mixtures at 298 K and 1 atm, as a function of the mole fraction of MeOH, X_{MeOH}, from MD simulations: (A) densities ρ, (B) dielectric permittivities $\epsilon(0)$, (C) excess volume of mixing ΔVOL_{mix} and (D) excess potential energy of mixing ΔU_{mix}. Experimental data are shown in solid lines and results of the CG simulations are in dashed lines.

s_m	s_T	$D_{Ca^{2+}}$ $[10^{-9}\mathrm{m^2s^{-1}}]$	$D_{SO_4^{2-}}$ $[10^{-9}\mathrm{m^2s^{-1}}]$	$\Delta g_{Ca^{2+}OW}\cdot 100$	$\Delta g_{SO_4^{2-}OW}\cdot 100$
1	1	1.06	1.23	0.00	0.00
	2	2.01	2.71	4.20	2.93
	3	4.11	6.03	8.59	6.71
	5	24.39	66.98	10.10	8.23
100	1	1.44	1.80	1.21	1.23
	2	13.22	16.89	1.25	1.20
	3	25.87	35.25	1.55	1.60
	5	51.64	74.56	1.60	2.11
200	1	1.23	1.46	1.34	1.11
	2	7.84	9.66	1.07	1.24
	3	15.27	18.87	1.45	1.40
	5	28.95	38.25	1.41	2.06
500	1	1.13	1.14	1.09	1.14
	2	4.22	4.48	1.18	1.18
	3	7.00	8.26	1.58	1.24
	5	13.19	15.83	1.47	1.97
1000	1	0.83	0.74	1.64	1.05
	2	2.33	2.51	1.75	1.19
	3	4.04	4.29	1.40	1.30
	5	7.43	7.96	1.70	1.54

TABLE 4.2. Configurational and dynamic properties of Ca^{2+} and SO_4^{2-} ions in aqueous solution from differently strong (s_m) adiabatically decoupled simulations in which the temperature of the ions is increased by different amounts (s_T). s_m: mass scaling factor, s_T: temperature scaling factor, D: diffusion coefficient, Δg: radial distribution difference.[46]

phenylethanolamine N-methyltransferase (PNMT) obtained using EDS and a GROMOS force field are compared to experimental data.[47] Excellent agreement with experiment is found.

4.6. Structure refinement based on NMR data

In structure refinement of proteins based on NMR data it is tried to find a single structure or a set of structures that reproduces the measured values of quantities such as NOE atom-atom distances bounds or ^{3}J-couplings. However, this is not always possible due to the presence of different conformers in solution. Such a case is illustrated in Fig. 4.6, where the set of NMR model structures deposited in the protein data bank for the peptide GCN4-p1 does not agree with the experimental NOE and ^{3}J-coupling data for this molecule. Using time-averaging refinement and a GROMOS force field the data can much better be reproduced[48,49].

4.7. Water configurations and mobility in the pore of a membrane protein

In Fig. 4.7, structures of the membrane protein OmpX embedded in a DMPC bilayer take from a simulation are shown[50], and Fig. 4.8 shows the water molecules trapped inside the β-barrel: a very stable salt-bridge and hydrogen-bond network exists in the barrel which inhibits a water flux.

4.8. Computer time required for MD simulation

Molecular dynamics computer simulations can be rather computer time demanding. In order to obtain an impression of the computing effort needed to simulate various biomolecular systems some benchmark data for GROMOS are given in Fig. 4.9.

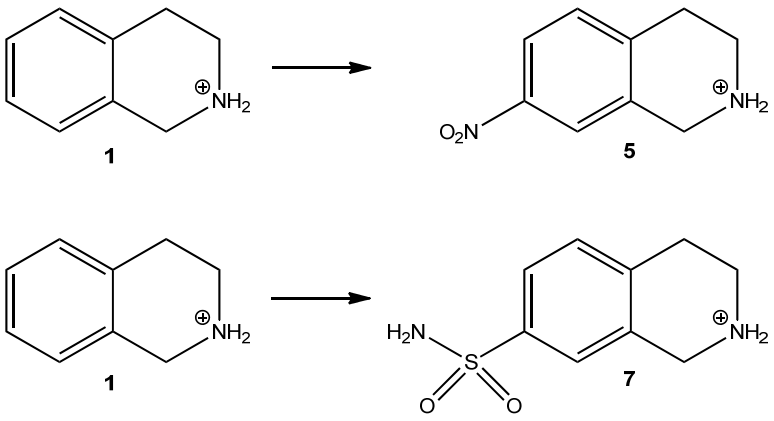

Pert.	$\Delta G^{complex}$	ΔG^{free}	$\Delta\Delta G^{binding}$(calc)	$\Delta\Delta G^{binding}$(exp)
1-5	-4.0 ± 0.9	6.2 ± 0.1	-10.2 ± 1.0	-10.3
1-7	-352.0 ± 2.0	-343.6 ± 0.2	-8.4 ± 2.2	-9.6

FIGURE 4.5. Perturbation between inhibitors 1 and 5, and 1 and 7 of the protein PNMT in water for the bound (complex) and unbound (free) ligands with the corresponding free enthalpy differences and the resulting relative binding free enthalpies as obtained from EDS simulations.[47]

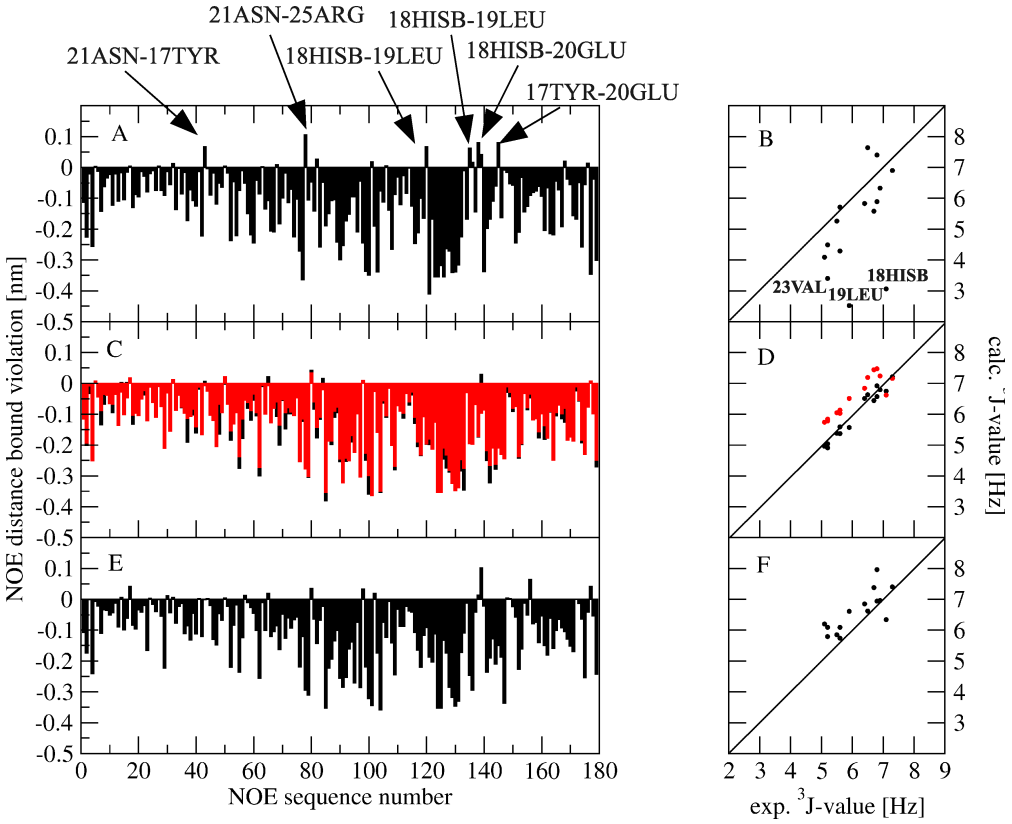

FIGURE 4.6. Deviations from the experimentally derived NOE upper distance bounds as a function of the NOE sequence number (left-hand panel, A) and comparison of the experimental and calculated ^{3}J(HN-HC$_\alpha$)-coupling constants (right-hand panel, B) for the 20 NMR model structures. The corresponding deviations (left-hand panel, C) and comparisons (right-hand panel, D) for the simulations in which time-averaged NOE distances (NOE_TAR) were restrained and either the ^3J-couplings were instantaneously restrained (3J_TAR) or a local-elevation biased sampling of torsional angles corresponding to ^3J-couplings were applied (3J_LE): NOE_TAR+3J_IR (black) and NOE_TAR+3J_LE (red). The corresponding deviations (left-hand panel, E) and comparisons (right-hand panel, F) for the weighted averages of the central members of the first ten conformational clusters of the NOE_TAR+3J_LE simulation. The 179 NOEs and 15 ^3J-couplings are defined in[48] .

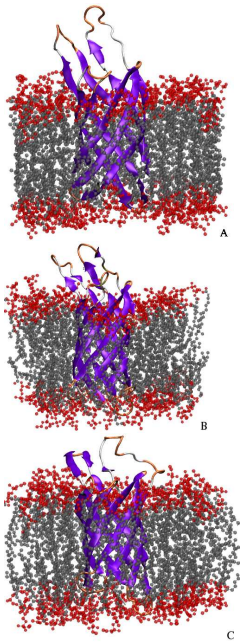

FIGURE 4.7. OmpX protein inserted in a lipid bilayer. A snapshot is shown at the beginning (a) and at the end of the simulations OmpX-DMPC-1 (b) and OmpX-DMPC-2 (c). The different colors indicate the secondary structure assignment. Lipid head groups are represented in red and lipid side chains in grey space-filling models.[50]

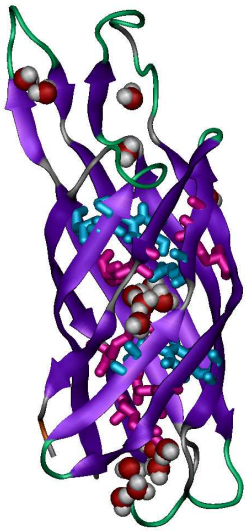

FIGURE 4.8. Water molecules trapped by hydrogen bonds inside the β-barrel for the OmpX-DHPC simulation[50] are shown as red and grey space-filling models. Residues for which intra-molecular hydrogen bonds are present for more than 90% or between 20 and 90% of the simulation time are drawn in pink or blue stick diagrams, respectively.

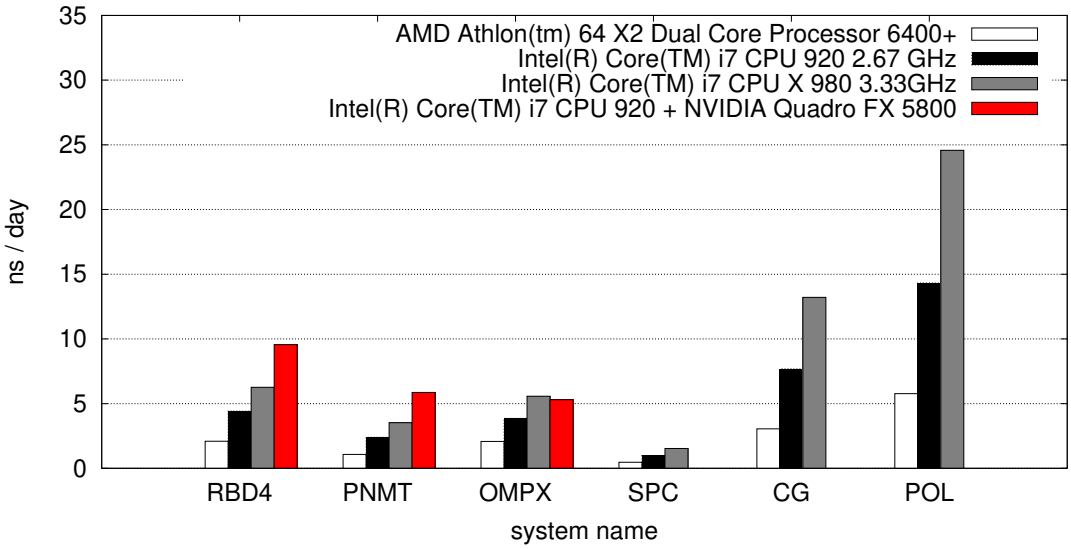

FIGURE 4.9. Benchmark results in nanoseconds per day for various biomolecular systems obtained on for different workstation class computers. Simulation settings: 2 fs integration time-step, twin-range cutoff scheme with cutoff values of 0.8 nm (short range) and 1.4 nm (long range). The pair list and long-range interactions were calculated every 5 steps. Systems: *RBD4*: polypyrimidine tract binding protein - RNA binding domain 4 bound to RNA CUCUCU, 1028 solute atoms, 5411 SPC solvent molecules. *PNMT*: phenylethanolamine N-methyltransferase (PNMT) protein with bound inhibitor, 2677 solute atoms, 9909 SPC solvent molecules. *OMPX*: Outer membrane protein X in a DPPC bilayer, 6322 solute atoms, 6559 SPC solvent molecules. *SPC*: 12800 SPC molecules treated as solute, 38400 atoms. *CG*: 2560 Coarse-grained water molecules, corresponding to 12800 fine-grained water molecules, 5120 solute atoms. *POL*: A beta heptapeptide in polarisable methanol, 63 solute atoms, 1095 polarisable MeOH molecules.

CHAPTER 5

Limitations of GROMOS

When applying MD to simulate a particular system, a number of preliminary questions have to be answered and choices related to the level of accuracy must be made. The *assumptions* and *approximations* that are made with respect to the molecular model and the computational procedures will determine the accuracy of the results obtained. Clearly there are *limitations* to the usefulness of application of simulation techniques. These will be briefly discussed below.

1. Since Newton's equations of motion are solved in an MD simulation, a *classical description* must be appropriate for the phenomena to be studied. Generally, when considering a molecular system at room temperature, quantum effects will not play a significant role as long as no covalent bonds are broken, etc.
2. With the use of modern computers the length of a MD simulation extends from a few tens of picoseconds up till hundreds of nanoseconds, depending on the size of the system. This means that the *time scale of a process* that can be simulated at the atomic level, is limited. For the simulation of activated processes special techniques are available, which require the pathway of the process to be known.
3. Only a limited *number of atoms* can be simulated, typically up till 10^5 atoms. The question is how many atoms are essentially involved in the phenomena to be studied. Atomic degrees of freedom that are not essential for an adequate description of the phenomenon being studied, may be removed by applying constraints, or stochastic techniques in combination with potentials of mean force, or the extended wall region boundary condition.
4. Last but not least, the *interaction function* or *force field* that is used will determine the accuracy of the obtained simulation results. A great variety of molecular models and force fields for molecular systems under various conditions is available. The choice of a particular force field should depend on the system properties one is interested in. Some applications require more refined force fields than others. Moreover, there should be a balance between the level of accuracy or refinement of different parts of a molecular model. Otherwise the computer effort put into a very detailed and accurate part of the calculation may easily be wasted due to the distorting effects of the crude parts of the model.

Although computer simulation is a very powerful technique to study the properties of molecular systems at the atomic level, one should bear in mind the various assumptions and approximations that are made and be aware of the limitations of the method.

Bibliography

[1] J. Hermans, H.J.C. Berendsen, W.F. van Gunsteren, and J.P.M. Postma. A Consistent Empirical Potential for Water-Protein Interactions. *Biopolymers*, 23:1513–1518, 1984.

[2] W.F. van Gunsteren and M. Karplus. Effect of Constraints on the Dynamics of Macromolecules. *Macromolecules*, 15:1528–1544, 1982.

[3] L.J. Smith, A.E. Mark, C.M. Dobson, and W.F. van Gunsteren. Comparison of MD simulations and NMR experiments for hen lysozyme: Analysis of local fluctuations, cooperative motions and global changes. *Biochemistry*, 34:10918–10931, 1995.

[4] X. Daura, A.E. Mark, and W.F. van Gunsteren. Parametrization of Aliphatic CHn United Atoms of GROMOS96 Force Field. *J. Comput. Chem.*, 19:535–547, 1998.

[5] L.D. Schuler and W.F. van Gunsteren. On the Choice of Dihedral Angle Potential Energy Functions for n-Alkanes. *Mol. Simul.*, 25:301–319, 2000.

[6] L.D. Schuler, X. Daura, and W.F. van Gunsteren. An Improved GROMOS96 Force Field for Aliphatic Hydrocarbons in the Condensed Phase. *J. Comput. Chem.*, 22:1205–1218, 2001.

[7] I. Chandrasekhar, M. Kastenholz, R.D. Lins, C. Oostenbrink, L.D. Schuler, D.P. Tieleman, and W.F. van Gunsteren. A consistent potential energy parameter set for lipids: Dipalmitoylphosphatidylcholine as a benchmark of the GROMOS96 45A3 force field. *Eur. Biophys. J.*, 32:67–77, 2003.

[8] C. Oostenbrink, A. Villa, A.E. Mark, and W.F. van Gunsteren. A biomolecular force field based on the free enthalpy of hydration and solvation: the GROMOS force-field parameter sets 53A5 and 53A6. *J. Comput. Chem.*, 25:1656, 2004.

[9] T.A. Soares, P.H. Hünenberger, M.A. Kastenholz, V. Kräutler, T. Lenz, R.D. Lins, C. Oostenbrink, and W.F. van Gunsteren. An Improved Nucleic-Acid Parameter Set for the GROMOS Force Field. *J. Comput. Chem.*, 26:725–737, 2005.

[10] R.D. Lins and P.H. Hünenberger. A new GROMOS force field for hexopyranose-based cardohydrates. *J. Comput. Chem.*, 26:1400–1412, 2005.

[11] M. Winger, A.H. de Vries, and W.F. van Gunsteren. Force-field dependence of the conformational properties of alpha,omega-dimethoxypolyethylene glycol. *Mol. Phys.*, 107:1313–1321, 2009.

[12] D. Poger, W.F. van Gunsteren, and A.E. Mark. A new force field for simulating phosphatidylcholine bilayers. *J. Comput. Chem.*, 31:1117–1125, 2010.

[13] H. Hansen and P.H. Hünenberger. A reoptimized GROMOS force field for hexopyranose-based carbohydrates accounting for the relative free energies of ring conformers, anomers, epimers, hydroxymethyl rotamers and glycosidic linkage conformers. *J. Comput. Chem.*, 32:998–1032, 2011.

[14] N. Schmid, A. P. Eichenberger, A. Choutko, S. Riniker, M. Winger, A.E.. Mark, and W.F. van Gunsteren. Definition and testing of the GROMOS force-field versions: 54A7 and 54B7. *Eur. Biophys. J.*, 40:843–856, 2011.

[15] M.M. Reif, P.H. Hünenberger, and C. Oostenbrink. New interaction parameters for charged amino acid side chains in the GROMOS force field. *J. Chem. Theory Comput.*, 8:3705–3723, 2012.

[16] W.F. van Gunsteren, S.R. Billeter, A.A. Eising, P.H. Hünenberger, P. Krüger, A.E. Mark, W.R.P. Scott, and I.G. Tironi. *Biomolecular Simulation: The GROMOS96 Manual and User Guide*. Vdf Hochschulverlag AG an der ETH Zürich, Zürich, Switzerland, 1996.

[17] D.P. Geerke and W.F. van Gunsteren. Force Field Evaluation for Biomolecular Simulation: Free Enthalpies of Solvation of Polar and Apolar Compounds in Various Solvents. *ChemPhysChem*, 7:671–678, 2006.

[18] H.J.C. Berendsen, J.P.M. Postma, W.F. van Gunsteren, and J. Hermans. Interaction models for water in relation to protein hydration. In B. Pullman, editor, *Intermolecular Forces*, pages 331–342. Reidel, Dordrecht, 1981.

[19] A. Glättli, X. Daura, and W.F. van Gunsteren. Derivation of an improved SPC model for liquid water: SPC/A and SPC/L. *J. Chem. Phys.*, 116:9811–9828, 2002.

[20] R. Walser, A.E. Mark, W.F. van Gunsteren, M. Lauterbach, and G. Wipff. The effect of force-field parameters on properties of liquids: Parametrization of a simple three-site model for methanol. *J. Chem. Phys.*, 112:10450–10459, 2000.

[21] D.P. Geerke, C. Oostenbrink, N.F.A. van der Vegt, and W.F. van Gunsteren. An Effective Force Field for Molecular Dynamics Simulations of Dimethyl Sulfoxide and Dimethyl Sulfoxide-Water Mixtures. *J. Phys. Chem. B*, 108:1436, 2004.

[22] I.G. Tironi and W.F. van Gunsteren. A molecular dynamics simulation study of chloroform. *Mol. Phys.*, 83:381–403, 1994.

[23] I.G. Tironi, P. Fontana, and W.F. van Gunsteren. A molecular dynamics simulation study of liquid carbon tetrachloride. *Mol. Simul.*, 18:1–11, 1996.

[24] L.J. Smith, H.J.C. Berendsen, and W.F. van Gunsteren. Computer Simulation of Urea-Water Mixtures: A Test of Force Field Parameters for Use in Biomolecular Simulations. *J. Phys. Chem. B*, 108:1065–1071, 2004.

[25] P.J. Gee and W.F. van Gunsteren. Acetonitrile revisited: a molecular dynamics study of the liquid phase. *Mol. Phys.*, 104:477–483, 2006.

[26] H. Yu, D.P. Geerke, H. Liu, and W.F. van Gunsteren. Molecular dynamics simulations of liquid methanol and methanol-water mixtures with polarizable models. *J. Comput. Chem.*, 27:1494–1504, 2006.

[27] D.P. Geerke and W.F. van Gunsteren. The performance of non-polarizable and polarizable force-field parameter sets for ethylene glycol in molecular dynamics simulation of the pure liquid and its aqueous mixtures. *Mol. Phys.*, 105:1861–1881, 2007.
[28] D.P. Geerke and W.F. van Gunsteren. On the calculation of atomic forces in classical simulation using the charge-on-spring method to explicitly treat electronic polarisation. *J. Chem. Theory Comput.*, 3:2128–2137, 2007.
[29] D.P. Geerke and W.F. van Gunsteren. Calculation of the free energy of polarization: quantifying the effect of explicitly treating electronic polarization on the transferability of force-field parameters. *J. Phys. Chem. B*, 111:6425–6436, 2007.
[30] A.P. Kunz and W.F. van Gunsteren. Development of a non-linear classical polarisation model for liquid water and aqueous solutions: COS/D. *J. Phys. Chem. A*, 113:11570–11579, 2009.
[31] Z. Lin, A.P. Kunz, and W.F. van Gunsteren. A one-site polarizable model for liquid chloroform: COS/C. *Mol. Phys.*, 108:1749–1757, 2010.
[32] A.P.E. Kunz, A.P. Eichenberger, and W.F. van Gunsteren. A simple, efficient polarisable molecular model for liquid carbon tetrachloride. *Mol. Phys.*, 109:365–372, 2011.
[33] O.M. Szklarczyk, S.J. Bachmann, and W.F. van Gunsteren. A polarisable empirical force field for molecular dynamics simulation of liquid hydrocarbons. *J. Comput. Chem.*, 35:789–801, 2014.
[34] S.J. Bachmann and W.F. van Gunsteren. Polarisable model for DMSO and DMSO-water mixtures. *J. Phys. Chem. B*, 118:10175–10186, 2014.
[35] S.J. Bachmann and W.F. van Gunsteren. On the compatibility of polarisable and non-polarisable models for liquid water. *Mol. Phys.*, 112:2761–2780, 2014.
[36] S.J. Bachmann and W.F. van Gunsteren. An improved polarisable water model for use in biomolecular simulation. *J. Chem. Phys.*, 141:22D515, 2014.
[37] Z. Lin, S.J. Bachmann, and W.F. van Gunsteren. GROMOS polarisable charge-on-spring models for liquid urea: COS/U and COS/U2. *J. Chem. Phys.*, 142:094117, 2015.
[38] S. Riniker and W.F. van Gunsteren. A simple, efficient polarisable coarse-grained water model for molecular dynamics simulations. *J. Chem. Phys.*, 134:084110, 2011.
[39] O. Szklarczyk, E. Arvaniti, and W.F. van Gunsteren. Polarisable coarse-grained models for molecular dynamics simulation of liquid cyclohexane. *J. Comput. Chem.*, 36:1311–1321, 2015.
[40] A.P. Eichenberger, W. Huang, S. Riniker, and W.F. van Gunsteren. A supra-atomic coarse-grained GROMOS force field for aliphatic hydrocarbons in the liquid phase. *J. Chem. Theory Comput.*, 11:2925–2937, 2015.
[41] J.R. Allison, S. Riniker, and W.F. van Gunsteren. Coarse-grained models for the solvents dimethyl sulfoxide, chloroform and methanol. *J. Chem. Phys.*, 136:054505, 2012.
[42] W. Huang, S. Riniker, and W.F. van Gunsteren. Rapid sampling of folding equilibria of β-peptides in methanol using a supramolecular solvent model. *J. Chem. Theory Comput.*, 10:2213–2223, 2014.
[43] W. Huang, N. Hansen, and W.F. van Gunsteren. On the use of a supramolecular coarse-grained model for the solvent in simulations of the folding equilibrium of an octa-β-peptide in MeOH and H2O. *Helv. Chim. Acta*, 97:1591–1605, 2014.
[44] S. Riniker, A.P.E. Kunz, and W.F. van Gunsteren. On the calculation of the dielectric permittivity of molecular models in the liquid phase. *J. Chem. Theory Comput.*, 7:1469–1475, 2011.
[45] Z. Lin, N. Schmid, and W.F. van Gunsteren. The effect of using a polarizable solvent model upon the folding equilibrium of different beta-peptides. *Mol. Phys.*, 109:493–506, 2011.
[46] A.P.E. Kunz and W.F. van Gunsteren. Enhancing the configurational sampling of ions in aqueous solution using adiabatic decoupling with translational temperature scaling. *J. Phys. Chem. B*, 115:2931–2936, 2011.
[47] S. Riniker, C.D. Christ, N. Hansen, A.E. Mark, P.C. Nair, and W.F. van Gunsteren. Comparison of enveloping distribution sampling and thermodynamic integration to calculate binding free energies of phenylethanolamine N-methyltransferase inhibitors. *J. Chem. Phys.*, 135:024105, 2011.
[48] J. Dolenc, J.H. Missimer, M.O. Steinmetz, and W.F. van Gunsteren. Methods of NMR structure refinement: molecular dynamics simulations improve the agreement with measured NMR data of a C-terminal peptide of GCN4-p1. *J. Biomol. NMR*, 47:221–235, 2010.
[49] J.H. Missimer, J. Dolenc, M.O Steinmetz, and W.F. van Gunsteren. Exploring the trigger sequence of the GCN4 coiled-coil: biased molecular dynamics resolves apparent inconsistencies in NMR measurements. *Protein Sci.*, 19:2462–2474, 2010.
[50] A. Choutko, A. Glättli, C. Fernández, C. Hilty, K. Wüthrich, and W.F. van Gunsteren. Membrane protein dynamics in different environments: simulation study of the outer membrane protein X in a lipid bilayer and in a micelle. *Eur. Biophys. J.*, 40:39–58, 2010.